EXPERIMENTAL CHARACTERIZATION OF PIEZOELECTRIC RADIAL FIELD DIAPHRAGMS FOR FLUIDIC CONTROL

R. G. Bryant[1], S. E. Kavli[2], R. A. Thomas, Jr.[3], K. J. Darji[4], K. M. Mossi[4]

[1]NASA Langley Research Center, MS 226, Hampton, VA 12681, USA
[2]NASA-USRP Student, University of North Dakota, Grand Forks, ND 58202, USA
[3]Raytheon Technical Services, Hampton, VA 23666, USA
[4]Virginia Commonwealth University, Richmond, VA 23284, USA

Abstract

NASA has recently developed a new piezoelectric actuator, the Radial Field Diaphragm or RFD. This actuator uses a radially-directed electric field to generate concentric out-of-plane (Z-axis) motion that allows this packaged device to be used as a pump or valve diaphragm. In order to efficiently use this new active device, experimental determination of pressure, flow rate, mechanical work, power consumption and overall efficiency needs to be determined by actually building a pump. However, without an optimized pump design, it is difficult to assess the quality of the data, as these results are inherent to the actual pump. Hence, separate experiments must be conducted in order to generate independent results to help guide the design criteria and pump quality. This paper focuses on the experiments used to generate the RFD's operational parameters and then compares these results to the experimentally determined results of several types of ball pumps. Also discussed are how errors are inherently introduced into the experiments, the pump design, experimental hardware and their effects on the overall system efficiency.

Keywords: Piezoelectric Pumps, Radial Field Diaphragms, Piezoelectric Actuators, NASA RFD

Introduction

Since the early 1990s, research and development of non-resonant piezoelectric pumps has been slow as indicated by the frequency of publications and products [1-5]. The advantages of using a non-resonant piezo-driven pump are the design of passive valves (ball and flapper) is simplified, increased range of useable frequencies with lower heat generation and reduced noise. The disadvantages are lower electrical/mechanical "E/M" efficiency when the pump is working under non-resonance conditions. The most popular actuator technologies used in piezoelectric pumps are the circular unimorph and bimorph-type diaphragms. These elements offer the advantage of the ability to compliantly seal about their perimeter with a slight sacrifice in performance. The drawbacks of these devices are that the diaphragms must be electrically insulated from the fluidic medium and the exposed ceramic is more prone to physical damage. Recently NASA Langley introduced a new type of piezoelectric actuator, the Radial Field diaphragm, "RFD" that addresses some of these issues [6-7]. The RFD, like the unimorph and bimorph, is a Z-axis actuator that is configured using an interdigitated-type electrode architecture encased in a fully sealed package. This type of arrangement offers several advantages; the piezo-ceramic and conductor are fully insulated from the environment, the electrode pattern affords a much lower capacitive load and the package provides a convenient mounting surface that allows for non-compliant fixturing. In order to evaluate these new pump designs, several parameters must be accounted for, the valves, the waveform used, the inherent design of the pump and the overall load parameters of the diaphragm itself. Since all these variables are coupled together, methods must be developed to isolate the parameters in order to judge their additive effects on the system. This paper describes the effect of the materials used for the ball valves and the experiments used to calculate the overall pump E/M efficiency and the diaphragm force as a function of pressure loading.

Experimental

Parts and Materials

The unelectroded PZT ceramics were obtained from CTS Wireless Inc. The epoxy adhesive used was E-120HP from Loctite Corp. The polyimide/copper clad used was Pyralux LF 8510 from Dupont Inc., and the release film and press pads were obtained from Pacothane Technologies Inc. The plastic hose fittings and balls were obtained from Small Parts Inc., the acrylic rod stock was from Norva Plastics Inc., and the burets were obtained from Fisher Scientific Inc.

RFD Fabrication Procedure

1) Assembly of Components: The materials were cleaned by wiping with ethanol using a lint-free

cloth and handled with latex gloves to prevent contamination. Adhesive was applied across both top and bottom copper side of the electrode patterned Pyralux sheets. The wafers were placed on the bottom electrode patterns and the top and bottom electrode patterns were then centered about the wafers. Trapped air pockets were removed by carefully applying pressure to the resulting laminate.
2) Curing Process: A metal plate was placed on a level surface, one press pad was placed on top of the plate followed by one sheet of release film and the assembled laminate. On this lay-up was placed another layer of release film another press pad and a second metal plate. The assembly was placed in a vacuum press for 10 minutes with the platens open and the vacuum on. The press was heated to 120°C and ~700 MPa pressure was applied for 1 hour. The press was cooled with the pressure and vacuum released prior to removal of the actuators.
3) Pump Housing: The single sided diaphragm pump "SSDP" housing was made from machined acrylic rod stock using standard carbide tooling.

Characterization
The displacement versus pressure data was acquired with the use of a Newport 850F LVDT, a Trek Model 609E-6 high voltage amplifier, and an Agilent 33210A waveform generator configured for DC output. All RFD's were measured while constrained in a watertight fixture where water pressure was applied to one side of the RFD, via a large buret, to induced displacement. The SSDPs were powered with a Trek Model 609E-6 high voltage amplifier controlled from an Agilent 33210A waveform generator using sinusoid waveforms. Electrical power was determined with a Tekronix TDS 210 O-Scope from voltage and current measurements. The SSDP flow rates, head pressure and power output were determined using water filled burets connected to the pump input and output manifold terminals.

Results and Discussion

Four sets of RFD wafers used in this work were based on CTS 3195HD (PZT-5A type) ceramic disks, 125 and 250 µm thick of 2.3 and 3.2 cm diameter. The electrode patterns (4/12 architecture) were two 20 µm thick x 100 µm wide copper intercirculating spiral traces spaced 200 µm apart and bonded to both faces of the piezoelectric disk. During poling, the RFDs deform into a conical shape. The application of a positive bias generates an upward displacement; a negative bias affords downward movement (flattening) of the actuator.
The first experiment involved generating pressure (or force) versus displacement plots. Since the RFD is a curved actuator, point loading the device would generate results that could not be correlated to the intended application. Thus, a water pressure cell (Fig. 1) was designed and configured, (Fig. 2) to generate pressure. Filling the buret and sealed chamber, and letting the water exit through the outlet, until the proper water height was obtained in the buret zeroed the system's water pressure.

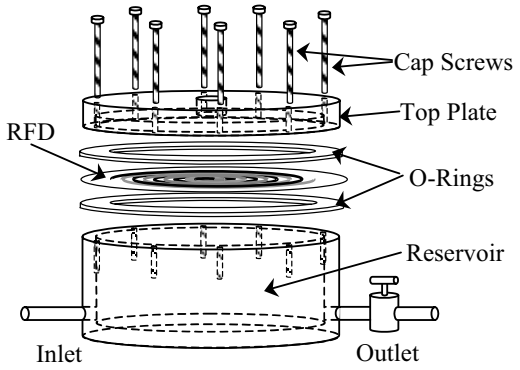

Fig. 1: *Exploded Schematic of RFD Water Pressure Cell*

Pressure versus displacement curves were generated by weighing the amount of water added to the buret, from the zero load line. At each addition of water, the RFD was incrementally forced upward (indicated by LVDT) in response to the applied pressure, and a negative DC potential was then applied to the RFD to force it down to its original position (indicated by the LVDT). This was done until either the RFD could not move (block pressure) or the further application of negative voltage would cause the RFD to repole.

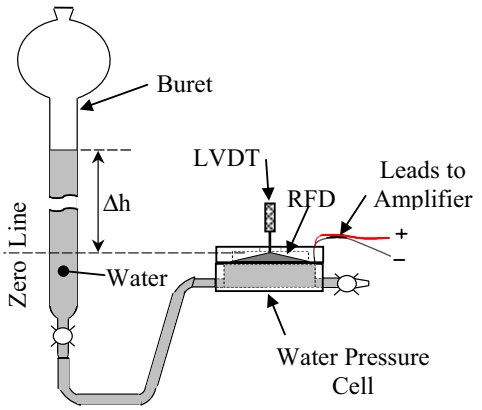

Fig. 2: *Test Setup Used to Calculate Pressure or Force vs. Displacement.*

The maximum negative voltage that can be applied to the RFDs without the risk of repoling under quasi-isostatic conditions is -500 volts, based on the line architecture. Hence, any pressure compensation exceeding -500 VDC was not done. The results of the displacement versus pressure (force) were plotted in Figs. 3 and 4.

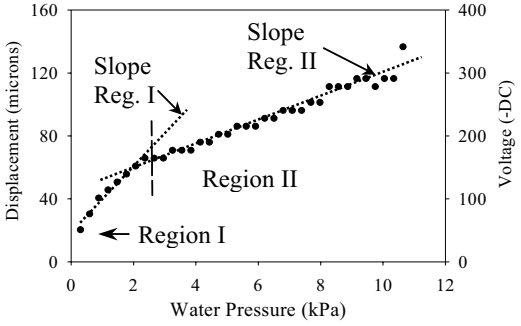

Fig. 3: *Example of Pressure vs Displacement and –DCV for 125 µm x 2.3 cm dia. RFD*

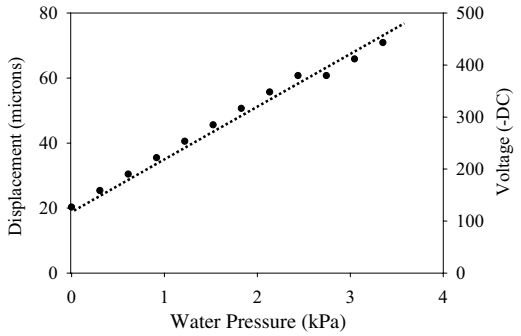

Fig. 4: *Example of Pressure vs Displacement and –DCV for 125 µm x 3.2 cm dia. RFD.*

The Pressure versus Displacement curves for the 2.3 cm dia. RFD displayed two linear regions (Fig. 3), whereas the plots for the 3.2 cm dia. actuators were linear (Fig. 4). The first region "R I" of the curve (Fig. 3) is where the water pressure does not exert much force on the RFD. The second region "R II" is where the RFD is physically strained by the pressure, and may elastically stretch the actuator package and the water cell's O-rings. By extrapolating the first and second partitioned slopes of the Pressure vs. Displacement line to -500 VDC. The estimated block pressure and force are then approximated; the calculated force is the pressure multiplied the actuator area Table 1.

Table 1: RFD Block Pressures

RFD geometry (thickness x dia.)	BP(kPa):BF(N) R I	BP(kPa):BF(N) R II
125 µm x 2.3 cm	7.0 : 11.6	24.5 : 40.7
250 µm x 2.3 cm	9.8 : 16.3	21.6 : 35.8
125 µm x 3.2 cm	2.6 : 8.5	2.6 : 8.5
250 µm x 3.2 cm	3.4 : 10.9	3.4 : 10.9

BP = Block Pressure : BF = Block Force

The second part of the investigation involved the building and assembling two prototype SSDPs that allow the different balls and RFDs to be easily interchanged (Fig. 5).

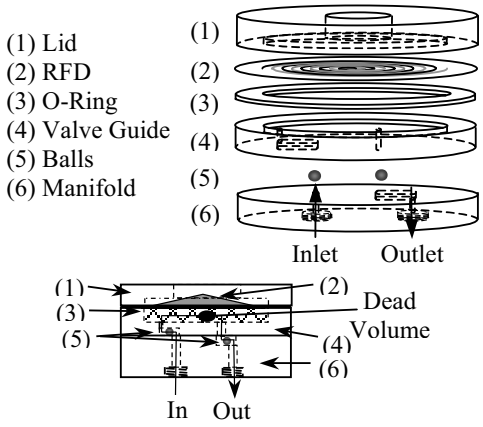

Fig. 5: *Exploded and Assembled Schematic of SSDPs*

The five types of balls used were all 1.6 mm dia. and of the following materials/densities in g/cc; acetal/1.4, aluminum oxide/3.75, chrome steel/7.47, brass/8.85 and tungsten carbide/18.8. The setup for testing the SSDPs is shown in Fig. 6.

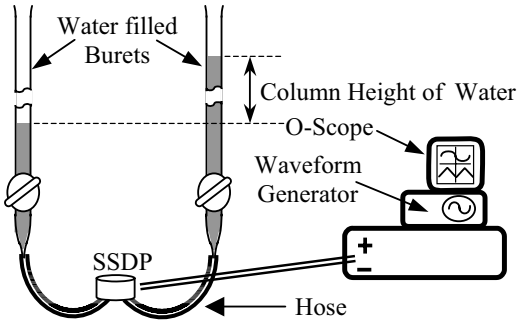

Fig. 6: *Test Setup for SSDPs*

There are several characteristics that contribute to the efficiency of a passive valve driven diaphragm pump. The diaphragm controls the valves through the force exerted on the medium via displacement and velocity. The waveform affects the velocity of the diaphragm; a wave has two points per cycle where diaphragm acceleration and velocity are nearly zero. This can cause the valves to float and become influenced by the fluidic pressure. Also, the input waveform may not be the same as the resulting pressure waveform that acts on the fluid. Other factors include the ball and fluid densities, fluid viscosity, hose diameter and length, the internal pump channels and dead volume, valve travel, wettability of the materials, and use of one or both sides of the diaphragm. The operating frequency of the pump is a function of the valves. Running the SSDPs at several frequencies and noting the column height after 2 min. determined the optimal operating frequency of ~4-5 Hz. The results shown in Fig. 7 are of the 2.3 cm dia. 125 µm RFD SSDP with different balls, while Fig. 8 and Table 2 display the best results obtained from the 2.3 and 3.2 SSDPs.

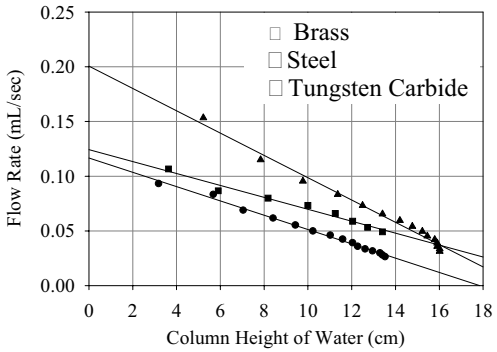

Fig. 7: *Flow Rate vs. Column Height for SSDP 125 µm x 2.3 cm dia. RFDs run at 4 Hz.*

The balls made from acetal and alumina had a tendency to stick in the pumps. The metal balls proved to be much more suitable.

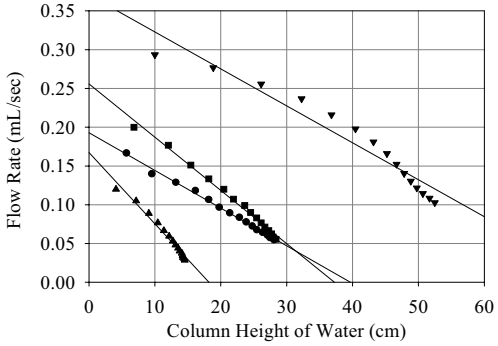

Fig. 8: *SSDP Best Performance Data – see Table 2 for Key:*

Table 2: Fig. 8 Key.

RFD in SSDP	Ball Material	Freq. Hz
□ - 3.2 cm dia x 125 µm	Chrome Steel	4
□ – 2.3 cm dia x 250 µm	Brass	5
□ – 2.3 cm dia x 125 µm	Chrome Steel	4
□ - 3.2 cm dia x 250 µm	Chrome Steel	4

The SSDPs were run for 15 minutes, and the column heights at time intervals were recorded, the back flow was minimized by design. This data was used to calculate mechanical power; the electrical power was calculated from the O-scope, to afford the E/M % efficiency of each SSDP. The block force of the RFDs was calculated from extrapolating the slope of the lines in Fig. 8 to the X-axis and comparing values with those of Table 1 (see Table 3).

Table 3: Calculated Properties of RFDs and SSDPs.

[1]SSDP/RFD	[2]BF (N) R I : R II	[3]BF (N)	E/M %
□	8.5 : 8.5	0.31	0.73
□	16.3 : 35.8	0.64	0.12
□	11.6 : 40.7	0.39	0.23
□	10.9 : 10.9	1.34	0.70

1) see Table 2. 2) see Table 1 for BF. 3) see Fig 8.

The general trend of the RFD and SSDP performance is that the thicker disks in each set afford the best results in terms of pressure. However, other trends can only be speculated at this time as the amount of uncorrelated variables mask the expected trends. This is reflected in the large difference of extrapolated block force values from the SSDP vs. Pressure test. One problem is the current RFD manufacturing process affords actuators that have a ±20% variance in performance. When this issue is resolved, increased precision in data trends will occur.

Conclusions

Several SSDP using the RFD as the active element were made with several types of ball valves. The chrome steel balls in the 3.2 cm. SSDP performed the best. However, the estimated force generated by the pumps was much less that that approximated from the pressure test. This is an indication of the inefficiencies associated with, a non-optimized pump design, drive electronics and RFD fabrication. Future work in this area will focus on RFD manufacturing, generating work functions from a modified pressure test and optimizing the pump design.

References

[1] R. G. Bryant, R. A. Thomas, Jr., D. L. Chattin, and. L. M. Pietruszka, "Radial field Diaphragm Piezoelectric Pumps", Ceramic Transactions, 105, 455, (2003).

[2] M. C. Carrozza, N. Croce, B. Magnani and P. Dario, "A piezoelectric-driven stereolithography-fabricated micropump," J. Micromech. Microeng., 5, 177, (1995).

[3] D. Accoto, M. C. Carrozza and P. Dario, "Modeling of micropumps using unimorph piezoelectric actuator and ball valves," *J.* Micromech. Microeng., 10, 277, (2000).

[4] S. Böhm, W. Olthuis and P. Bergveld, "A plastic micropump constructed with conventional techniques and materials," Actuators and Sensors, 77, 223, (1999).

[5] J. A. Waanders, "Piezoelectric Ceramics, Properties and Applications," *Philips Components*, (1991).

[6] R. G. Bryant, R. T. Effinger IV, and B. M. Copeland Jr., "Radial Field Piezoelectric Diaphragms," Actuator 2002, 8th International Conf. on New Actuators, 49, Bremen, Germany (2002).

[7] R. G. Bryant, R. T. Effinger IV, I. Aranda Jr., B. M. Copeland Jr., E. W. Covington III, and J. M. Hogge, "Radial Field Piezoelectric Diaphragms," J. Intelligent Material Systems and Structures, (2004) in Press.